DOI: 10.14529/jsfi250407

Novel Oxygen-Deficient Centers and Other Intrinsic Defects in Amorphous SiO_2: Quantum Molecular Dynamics Simulations

Vladimir B. Sulimov[1], *Danil C. Kutov*[1], *Alexey V. Sulimov*[1], *Fedor V. Grigoriev*[1], *Alexander A. Tikhonravov*[1]

The formation of stoichiometric and oxygen-deficient amorphous states of a-SiO_2 from a corresponding crystal was simulated using the melting-quenching procedure. To simulate the entire process, quantum molecular dynamics implemented in the VASP program and supercells containing 64 Si atoms and 128 O atoms were used. This size allows modeling the formation of rings with a small number of Si–O–Si bridges. At given heating and cooling rates of 0.5 K/fs, the transformation of the crystal's atomic network into a disordered structure was studied depending on the melt stabilization temperature. It is shown that despite the strong change in the topology of the atomic network in a-SiO_2 compared to the crystal, the bulk of the atoms constitute a continuous network of SiO_4 tetrahedra linked by oxygen vertices. Local disturbances of this arrangement of atoms are intrinsic point defects of SiO_2, which are given special attention. It has been shown that most of the defects present in oxygen-deficient states are also present in stoichiometric states of a-SiO_2. Along with the known intrinsic defects of SiO_2, new defects were also identified, including those associated with oxygen deficiency. It is shown that for two generally accepted models of oxygen-deficient centers (ODCs) in a-SiO_2, the energy of formation of an oxygen vacancy is significantly lower than the energy of formation of a twofold coordinated silicon atom. The point defects of a-SiO_2 identified in this work create a foundation for the interpretation of experimental data on the radiation resistance of optical fibers, the effects of high-power laser radiation on optical coatings, and in microelectronics, where insulating layers based on a-SiO_2 are used.

Keywords: quantum molecular dynamics, amorphous SiO_2, point defects, oxygen deficiency, oxygen vacancy, ODC.

Introduction

Amorphous silica or a-SiO_2 and silica glass or quartz glass are names of disordered states of silicon dioxide. This non-crystalline material has unique properties and is widely used in microelectronics for insulating layers in most of semiconductor devices, in high-speed communication lines as a base component of optical fibers, in multilayer optical coating as low-refractive index thin films, and in many other applications. The structure of perfect a-SiO_2 at the atomic level is usually imagined as a disordered framework of SiO_4-tetrahedra bound to each other by common oxygen atoms in the tetrahedra vertexes. Many different silicon dioxide crystalline polymorphs (quartz, cristobalite, tridymite, coesite) have such structure with different packing of SiO_4-tetrahedra. Perfect silicon dioxide in its crystalline or amorphous form has one of the widest transparency windows, the band gap, about 9 eV. Disruptions to the ideal network of interatomic bonds in pure a-SiO_2 are called intrinsic point defects, and some of them are associated with electron states in the band gap. Existence of these states narrows the transparency window and results in absorption of the light irradiation with photon energies below 9 eV. This absorption leads to additional losses in optical fibers and decreases the laser damage threshold of optical coating. Band gap states of point defects play a role of hole or electron traps creating radiation-induced color centers in silica-based fibers [1] and different phenomena in semiconductor devices such as interface charge, leakage current, *etc.* [21].

[1]Research Computing Center of Lomonosov Moscow State University, Moscow, Russian Federation

Among silica intrinsic point defects, oxygen-deficient centers or ODCs are most widely discussed as precursors of various radiation-induced color and/or ESR-active centers, ESR – Electron Spin Resonance. ODCs also play a key role in the formation of the UV-written refractive index gratings in Ge-doped silica-based fibers [23]. Authors of various publications use two ODC models to interpret the phenomena observed in silicon dioxide: the oxygen vacancy, ODC(I), and the twofold coordinated silicon atom, ODC(II) or =Si, where the symbol "=" denotes two Si–O bonds that connect the silicon atom to the rest of the SiO_4-tetrahedra network. Note that the stoichiometry of the SiO_2 supercell with an oxygen vacancy is equal to the stoichiometry of the SiO_2 supercell with a =Si defect. The oxygen vacancy model refers to a common defect in crystals, but =Si originally relates to a defect at silica surface. Oxygen vacancies have been discussed as models for various defects in quartz glass, including ODC models, and corresponding calculations have been carried out for over 50 years, *e.g.* see [3, 25, 27] and references therein. The model of ODC in the form of a twofold coordinated silicon atom =Si was introduced much later [16, 19], but is currently being discussed for the interpretation of experimental data along with the oxygen vacancy [6, 14].

Despite the more or less general acceptance of these two models, the existence of oxygen vacancies and =Si atoms in a-SiO_2 is based only on indirect experimental evidences, since the atomistic structure of point defects can only be obtained by analyzing ESR spectra, but ODCs do not manifest themselves in ESR. Therefore, we decided to obtain direct evidence for the existence of these ODC models using atomistic computer simulations.

We recently performed quantum molecular dynamics simulations of amorphous silica using the melting-quenching procedure [22, 24] and found that in most cases, the resulting amorphous stoichiometric silicon dioxide does not contain oxygen vacancies or twofold coordinated silicon atoms. In these works, we used spin-unpolarized quantum MD calculations, which in general do not allow to describe adequately breaking and restoring interatomic bonds during the melting-quenching procedure.

In the present work, carried out with the aim of searching for possible intrinsic defects of a-SiO_2, the results of modeling stoichiometric and oxygen-deficient a-SiO_2 are described. Modeling was carried out using the same melting-quenching procedure as in [22, 24], but with spin-polarized calculations for a more adequate description of the breaking and restoring of Si–O bonds. We investigated more thoroughly than in works [22, 24] the transformation from the atomic lattice topology of the crystal to the more disordered atomic network topology of a-SiO_2. Oxygen deficiency was created in the initial crystal or a-SiO_2 by removing one or two oxygen atoms, creating single oxygen vacancies or divacancies. In this process, several dozen models of amorphous states of stoichiometric and oxygen-deficient a-SiO_2 were obtained, and the intrinsic point defects formed in them were identified, including 12 defects that can be attributed to oxygen deficiency. The obtained results allow us to take a different look at the models of oxygen-deficient centers in amorphous silicon dioxide and the mechanisms of their participation in various processes under ionizing or laser irradiation.

The article is organized as follows. Section 1 is devoted to the short description of the methods used for modeling amorphous states of silicon dioxide. In Section 2, we present results of modeling stoichiometric and oxygen-deficient amorphous states of SiO_2 and analysis of their point defects. Section 3 summarizes the results of the study, discusses the intrinsic point defects identified, particularly those related to oxygen deficiency, and highlightes some of the problems

encountered. Conclusion contains a brief summary of the results of the work, final conclusions and points the directions for further work.

1. Models and Methods

The method for obtaining amorphous states of SiO_2 involves modeling the melting-quenching process of a crystal using quantum molecular dynamics, MD. The VASP program [10] was used for modeling. β-cristobalite was used as the starting crystal, and the simulations were performed with its supercell containing 192 atoms (64 Si atoms and 128 O atoms) with periodic boundary conditions. The system was heated and cooled at a rate of 0.5 K/fs; the melt was stabilized at a given T_{melt} within 6 ps in most cases, which was sufficient to achieve temperature stabilization at T_{melt}. In some cases, the stabilization time at T_{melt} was significantly increased to compare the properties of the obtained amorphous states. After cooling the system to 300 K, it was stabilized for 12 ps, after which the supercell energy was optimized. In all cases of melting-quenching, the time of 12 ps was sufficient to stabilize energy of the system at 300 K. Molecular dynamics simulations were performed in the NPT ensemble when the number of atoms N, pressure P and temperature T were constant. In this modeling, the volume of the system was not fixed and could change in accordance with strong temperature changes during the melting-quenching process, which made it possible to avoid strong internal stresses in the system. During MD simulation and during energy optimization of the supercell, its volume and shape, and the positions of all atoms could change. The modeling methodology is described in more detail in the works [22, 24].

2. Results

Our previous studies using spin-unpolarized quantum MD calculations have shown that there is a narrow range of melt stabilization temperature T_{melt} above which amorphization of silicon dioxide crystals occurs during the melting-quenching procedure [22, 24]. Amorphization here refers to a change in the topology of the atomic network of silicon dioxide from a regular crystalline topology to a less ordered amorphous topology. One of the characteristic features of amorphous topology is the presence of low-membered rings built from Si–O–Si bridges formed by SiO_4-tetrahedra connected to each other by their oxygen vertices. For example, the high temperature β-cristobalite crystal contains only 6-membered rings, α-quartz contains 6- and 8-membered rings, but in amorphous silica there are also 3-, 4- and 5-membered rings [13, 31]. In our spin-unpolarized simulation, amorphization of an initial stoichiometric β-cristobalite crystal happens above $T_{melt} = 4700$ K. Therefore, we investigated non-stoichiometric compositions for several values of T_{melt} near 4700 K, but first we briefly present new results on amorphization of stoichiometric SiO_2, modelled by the melting-quenching procedure using spin-polarized quantum MD calculations (keyword ISPIN = 2 in VASP version 5.4.4 compiled for GPU).

2.1. Stoichiometric Amorphous States

Amorphous states of SiO_2 were obtained from β-cristobalite crystal using the melting-quenching procedure at different melt stabilization temperatures. The results are presented in Tab. 1, where for a-SiO_2-4800, the E_g value given in brackets corresponds to the transition of an electron with the second spin direction, and the designations of point defects are explained in the text below. For brevity, we will further denote, for example, as a-SiO_2-4700 the amorphous

state of silicon dioxide obtained by the melting-quenching procedure with stabilization of the melt at 4700 K for 6 ps.

Table 1. Stoichiometric SiO_2. Stabilization of the melt was 6 ps for all T_{melt}

Structure	Crystal	Amorphous SiO_2, T_{melt}, °K				
		4500	4600	4700	4800	4900
E_{opt}, eV	−1516.53	−1513.90	−1519.55	−1519.51	−1482.89	−1495.00
Defects	–	$2BO_3C$, ≡Si–O	–	–	=Si, OV, Si_5, 2BOC, $2BO_3C$, O_2	Si_5, O_3, 2BOC
R(Si–Si), $\mathring{A}$	3.10	2.47	3.16	3.10	3.00	3.19
ρ, g/cm^3	1.92	2.17	2.119	2.126	2.056	2.256
E_g, eV	5.35	2.31	5.56	5.55	3.42 (2.07)	3.41

In Tab. 1, E_{opt} represents the energy of the stoichiometric supercell after energy optimization from the crystal geometry or from the disordered state at the end of the melting-quenching procedure, R(Si–Si) is the distance between Si atoms adjacent to the oxygen atom that will be eliminated when creating an oxygen vacancy (see Section 2.2), ρ is the mass density of the system, E_g = E(LUMO) – E(HOMO), where E(LUMO) and E(HOMO) are energies of the lowest unoccupied and highest occupied molecular orbitals, respectively. The value of E_g estimates the lowest energy of electron excitations, for example, this is the width of the forbidden energy gap of the oxide crystal. However, if a supercell, crystalline or amorphous, contains several point defects with energies of electron states in the forbidden energy gap of the defect-free system, then the value of E_g, strictly speaking, cannot provide an estimate of the lowest excitation energy of the system, since the HOMO and LUMO states can belong to different point defects, widely separated in space, and the oscillator strength of the HOMO-to-LUMO transition in this case will be negligibly small. These considerations should be kept in mind when reading this article, in which, for the sake of completeness, we provide the values of E_g for all the cases considered.

Visual analysis of the position of atoms in the obtained amorphous supercells shows that at all melt stabilization temperatures T_{melt} up to and including 4400 K, the topology of the arrangement of atoms is the same as in the initial crystal with relatively small deviations of Si–O–Si angles from their values in the crystal. At T_{melt} = 4500 K, the first point defects appear. These are three following point defects. Two of them, are painted green and gray in Fig. 1. These defects are a 2-Bridging Oxygen Center (2BOC), which is two adjacent SiO_4-tetrahedra linked to each other by two oxygen vertices [22, 24], and associated with it a threefold coordinated oxygen atom O_3, respectively. The third defect is designated as ≡Si–O, where the symbol "≡" stands for three ordinary Si–O bonds with the remaining SiO_2 atomic network, and the oxygen atom has only one Si–O bond. This is a non-bridging oxygen atom.

One of the two oxygen atoms of 2BOC forms a third bond to a Si atom from another SiO_4-tetrahedron; hereinafter such a combination of 2BOC and O_3 is designated as $2BO_3C$, where the index "3" denotes the presence of a threefold coordinated oxygen atom O_3. In Tab. 1, for a-SiO_2-4500, the value of R(Si-Si) corresponds to the distance between two Si atoms that make up the $2BO_3C$ defect. The topology of the atomic network of other supercell regions of a-SiO_2-4500 is close to the crystal structure with some variations of Si–O–Si angles. Obviously,

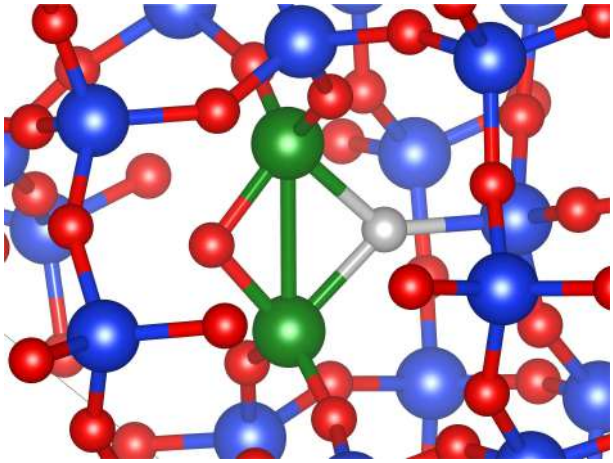

Figure 1. The $2BO_3C$ defect in a-SiO_2-4500; green balls are silicon atoms of the 2BOC defect, a grey ball is a threefold coordinated oxygen atom O_3

the 2BOC defect does not violate stoichiometry of the SiO_2 system. Also, two defects, $2BO_3C$ and ≡Si–O, do not violate stoichiometry of a-SiO_2-4500, which is expected, since the number of atoms in the supercell is constant in the MD simulations because we use the NPT ensemble, see Section 1. Indeed, the $2BO_3C$ center can be represented as a combination of the 2BOC center and a threefold coordinated silicon atom ≡Si. The latter in a combination with the ≡Si–O defect restore stoichiometry of SiO_2. The ≡Si–O defect has long been considered as a model for non-bridging oxygen hole center, the so-called NBOHC, which explains some optical absorption and luminescence bands in SiO_2 [15, 17, 18].

When the melt is stabilized at 4600 or 4700 K, then in the corresponding amorphous states, a-SiO_2-4600 and a-SiO_2-4700, the topology of the arrangement of atoms is again as in a defect-free crystal with small deviations of Si–O–Si angles from their crystalline values.

An increase in the duration of melt stabilization at T = 4700 K from 6 ps to 19 ps leads to a strong rearrangement of the topology of the atomic network, an increase in the energy of corresponding a-SiO_2-4700_19ps by more than 20 eV and the appearance of point defects: 2BOC, fivefold coordinated Si_5 and threefold coordinated ≡Si silicon atoms, which results in a sharp decrease of E_g to 2.02 eV due to the electron states of defects in the forbidden energy gap of SiO_2. The subscript "5" shows that the silicon atom has five Si–O bonds with five oxygen neighbors. The atomic network contains several four- and five-membered rings built from Si–O–Si bridges, which are absent in the crystal network. The ≡Si defect is a well known model of one of the most studied ESR active E′-centers in pure SiO_2 [5, 28].

The five Si–O bonds of Si_5 atoms are noticeably elongated to 1.68–1.85 $\AA$ compared to the length of the Si–O bonds of regular fourfold coordinated Si atoms 1.62–1.63 $\AA$ in the defect-free regions of the supercell; three adjacent oxygen atoms are located in the vertices of a triangle, in the center of which is the Si atom, and the other two adjacent oxygen atoms are at opposite ends of a straight line passing through the silicon atom perpendicular to the plane of the triangle. Note that from the stoichiometry point of view, the Si_5 defect is equivalent to one regular fourfold coordinated silicon atom forming a SiO_4-tetrahedron, and a ≡Si–O defect with a non-bridging oxygen atom.

At higher melt stabilization temperatures, a greater number of 2BOC defects and small rings built from three, four or five Si–O–Si bridges appear. Besides, some additional point

defects can be identified in a-SiO_2-4900 and a-SiO_2-4800. In a-SiO_2-4900, Si_5 and O_3 defects are found. Three Si–O bonds of length 1.77–1.89 $\AA$ of the O_3 defect are somewhat elongated comparing to a regular Si–O bond of 1.62 $\AA$. Note that from the stoichiometry point of view, the threefold coordinated oxygen atom O_3 is equivalent to the threefold coordinated silicon atom ≡Si, therefore, the O_3 defect can be classified as an oxygen deficient center (ODC) in the same way as the ≡Si. Also, a pair of defects Si_5 and O_3 corresponds to the stoichiometry of defect-free SiO_2.

The a-SiO_2-4800 supercell has two unpaired electrons from the triplet state of the interstitial oxygen molecule O_2, which appears during the melting-quenching process, and this amorphous state is significantly higher in energy than the other amorphous states we obtained, which do not have unpaired electrons. Also, there are a twofold coordinated silicon atom =Si, an oxygen vacancy in the form of ≡Si–Si≡ bond between two adjacent to the oxygen vacant site Si atoms with the Si–Si bond length 2.30 $\AA$, two Si_5 defects and two $2BO_3C$ defects. The presence of all these defects does not disturb the correct stoichiometry of SiO_2. Indeed, from the O_2 molecule, one oxygen atom binds to an oxygen vacancy and restores a regular oxygen bridge. Two Si_5 defects together with the =Si defect restore the stoichiometry of SiO_2, and two $2BO_3C$ centers give two ≡Si defects, which, together with the remaining oxygen atom, also restore the stoichiometry.

The Si–O bonds of the twofold coordinated silicon atom =Si are equal to 1.66 and 1.69 $\AA$, they are only slightly larger than the length of the regular Si–O bond in defect free regions. The angle O–Si–O is equal to 106.4°. An oxygen vacancy has the form of a ≡Si–Si≡ bond, which for brevity we will simply call the Si–Si bond.

An independent run of the melting-quenching procedure to obtain a-SiO_2-4800 again leads to a high energy state with two unpaired electrons. This amorphous state has an energy 3.86 eV lower and its mass density $\rho = 2.141$ g/cm^3 is slightly higher than the corresponding values of the a-SiO_2-4800 state presented in Tab. 1. However, in the new a-SiO_2-4800 state, there are no the =Si defect, oxygen vacancy, $2BO_3C$ and Si_5 defects, as well as the interstitial O_2 molecule, that were present in the previous a-SiO_2-4800 state. Instead, there are several 2BOC defects, several 3-, 4- and 5-membered rings, the ≡Si–O defect, and three threefold coordinated Si atoms: two Si atoms of the type ≡Si and one Si atom of the type =Si–O, the latter being a threefold coordinated Si atom, the third Si–O bond of which is linked to a non-bridging oxygen atom. One ≡Si atom has a pyramidal conformation with somewhat elongated Si–O bonds (1.63–1.68 $\AA$) and the other ≡Si atom has a planar conformation, in which the Si atom is in the plane of three adjacent oxygen atoms, with slightly shortened bond lengths (1.56–1.58 $\AA$). One unpaired electron is on the ≡Si atom with a pyramidal conformation and the second unpaired electron is on the non-bridging oxygen atom of the defect =Si–O. The Si–O bond of the non-bridging oxygen atom is noticeably shorter, 1.52 $\AA$, than other two bonds of this Si atom, the lengths of which are close to the length of regular Si–O bonds in silicon dioxide 1.62 $\AA$. In the latter a-SiO_2-4800 state, $E_g = 1.94$ and 1.51 eV for the excitation of electrons with different spins.

As can be seen from Tab. 1, the density of most of the obtained stoichiometric amorphous states, with the exception of the a-SiO_2-4900 state, is in the range of 2.10–2.17 g/cm^3, which corresponds to the results of our previously conducted spin-unpolarized calculations [22, 24]. The obtained values of the density of amorphous states are slightly lower than the experimental density of quartz glass 2.20 g/cm^3, and this small difference is within the errors of the PBE functional [8] and the PAW method [11].

As we can see in Tab. 1, the energy gap E_g of the crystal and of the defect free amorphous states a-SiO_2-4600 and a-SiO_2-4700 is about 5.4–5.6 eV. These values are much less than experimentally measured band gap of silicon dioxide, which is about 9 eV [2, 30]. This is a well know drawback of the PBE [8] functional and these values can be improved using PBE0 functional [12]. The formation of point defects leads to the appearance of electron states of defects in the SiO_2 forbidden gap and, as a consequence, to a significant decrease in the E_g values (see Tab. 1 for a-SiO_2-4800 and a-SiO_2-4900).

The conducted spin-polarized MD simulations resulted in practically the same amorphous states and their point defects as those obtained by spin-unpolarized quantum MD simulations [22, 24] using the melting-quenching procedure with the same parameters: melting and quenching rate, melt stabilization time, and stabilization time of the final amorphous state at 300 K. In addition, a new point defect =Si–O was discovered, which was not detected in the spin-unpolarized simulation. States with unpaired electrons, i.e., ESR-active states, were also obtained, which, however, are significantly higher in energy than the ESR-inactive states. With the same melting-quenching parameters, the use of spin-polarized calculations leads to amorphous states with a richer set of intrinsic defects than similar spin-unpolarized calculations, the results of which are presented in [22, 24].

Properties of amorphous states obtained from quartz crystal are close to the properties of amorphous states obtained from cristobalite crystal. In contrast to this, amorphization from stishovite crystal occurs at much lower temperatures due to instability of stishovite at normal pressure. Using the same melting-quenching procedure, we found that radical restructuring of the stishovite atomic network topology occurred at $T_{melt} = 3000$ K, when sixfold coordinated Si atoms and threefold coordinated oxygen atoms in the stishovite atomic network are transformed into a quartz glass network with fourfold and twofold coordinated Si and O atoms, respectively. Topology of atomic network of amorphous states obtained with $T_{melt} \geq 3000$ K from stishovite is, in general, the same as one of amorphous states obtained from cristobalite with the same set of possible point defects.

In the following research, we will carry out modeling of oxygen-deficient centers based on amorphous structures obtained from the cristobalite crystal. Three types of oxygen deficient centers ODCs are considered: a single oxygen vacancy OV, two spatially separated oxygen vacancies OV+OV, and an oxygen divacancy. Three methods of modeling are used: (**A**) ODC is created in a cristobalite crystal or in one of the above-obtained models of stoichiometric a-SiO_2, and then the energy of the corresponding supercell is optimized by changing its shape and volume, as well as the position of all its atoms; (**B**) ODC is created in the cristobalite crystal and then the melting-quenching procedure is carried out for different melt stabilization temperatures T_{melt}; (**C**) a supercell of a-SiO_2 created by the (**A**) approach with the corresponding ODC is subjected to the melting-quenching procedure with the same melt stabilization temperature that has been used in the preparation of the initial amorphous stoichiometric state.

2.2. Single Oxygen Vacancy, OV

A. Oxygen vacancy is created in existing stoichiometric states. The oxygen vacancy (OV) is created in the corresponding structure, cristobalite or amorphous (see Tab. 1), and then the energy of the supercell is optimized, and as a result of this, two adjacent to the vacant site silicon atoms relax to each other forming the Si–Si bond. Characteristics of the supercell with the oxygen vacancy are presented in Tab. 2. In a-SiO_2-4500, two types of oxygen vacancy were

created by removing one of the two oxygen atoms included in the $2BO_3C$ defect (Fig. 1). In Tab. 2, the 4500_2BOC column corresponds to the removal of the threefold coordinated oxygen atom, and the 4500_2BOC-1 column corresponds to the removal of the twofold coordinated oxygen atom from the $2BO_3C$ defect. In the table E_{opt}(OV) is the energy of the supercell with an oxygen vacancy after optimization, R(Si–Si) is the distance between Si atoms adjacent to the vacant oxygen site, E_g = E(LUMO) – E(HOMO), E_{form}(OV) is the formation energy of the oxygen vacancy calculated as follows: $E_{form}(OV) = E_{opt}(OV) + E(O) - E_{opt}$, where E_{opt} is the optimized energy of the supercell without oxygen vacancy (see Tab. 1), and E(O)= −1.897 eV is the energy of a single O atom obtained using spin-polarized calculations with the VASP program, ISPIN = 2, with the same PBE functionals and the same value of the ENCUT parameter that were used for the crystal and amorphous calculations presented in this report. If the oxygen vacancy is created in the defect free region of a-SiO_2-4500, then its properties are practically the same as those in defect free states a-SiO_2-4600 and a SiO_2-4700. Thus, for a-SiO_2-4500, an oxygen vacancy was created by removing an oxygen atom from the $2BO_3C$ defect that exists in the stoichiometric system.

Table 2. Main characteristics of oxygen vacancy created in crystalline or amorphous silicon dioxide supercell

Structure	Oxygen vacancy						
	Crystal	Amorphous SiO_2, T_{melt}, °K					
		4500_2BOC	4500_2BOC-1	4600	4700	4800	4900
E_{opt}(OV), eV	−1506.42	−1502.73	−1504.07	−1509.52	−1509.44	−1476.94	−1484.59
R(Si–Si), $\AA$	2.48	2.49	2.21	2.42	2.42	2.38	2.52
ρ, g/cm^3	1.92	2.18	2.16	2.12	2.12	2.14	2.27
E_{form}(OV), eV	8.22	9.27	7.93	8.13	8.18	7.92	8.51
E_g, eV	5.34	0.46	2.29	5.27	5.32	2.00	3.39

In cristobalite and all amorphous states, except those indicated in Tab. 2 as 4500_2BOC and 4500_2BOC-1, oxygen vacancies have the form of the Si–Si bond. The distances between silicon atoms adjacent to vacant oxygen sites vary in the range from 2.38 to 2.52 $\AA$ and are significantly smaller than distances between silicon atoms in regular Si–O–Si bridges of the defect-free region of silicon dioxide, indicating the formation of a strong Si–Si covalent bond. The variations of lengths of Si–Si bonds are apparently associated with some scattering of the positions of atoms in the immediate vicinity of the vacancies, caused by the structure of the amorphous state. The formation energy of the oxygen vacancy in the form of the Si–Si bond is in the range from 7.92 to 8.51 eV, and this scatter is also apparently due to some difference in the positions of the atoms in the vacancy environment. The formation energy of an oxygen vacancy created by removing an oxygen atom from the $2BO_3C$ defect is close to the above values for other amorphous states and the crystal, when a twofold coordinated oxygen atom is removed, but is slightly higher (9.27 eV) in the case of removing a threefold coordinated oxygen atom due to the breaking of three Si–O bonds.

The energy E_g for the cristobalite crystal and amorphous defect-free states a-SiO_2-4600 and a-SiO_2-4700 in the presence of an oxygen vacancy is only slightly less than the corresponding energy gap of defect-free supercells of stoichiometric compositions (see Tab. 1). This qualitatively corresponds to the excitation energy of the oxygen vacancy in quartz crystal 7.6 eV, calculated by an *ab initio* method [27]; this energy is in the vacuum UV region and is slightly less than the silicon dioxide forbidden energy gap [2, 30].

The structure of amorphous a-SiO_2-4700_19ps (the melt stabilized during 19 ps) contains a hand-created oxygen vacancy and the same defects that existed in this amorphous state before the creation of the oxygen vacancy. Comparing the values of E_g = 5.32 eV for a-SiO_2-4700 in Tab. 2 (here, apart from the vacancy, there are no other defects) and E_g = 2.06 eV for a-SiO_2-4700_19ps, it is clear that such a strong decrease in E_g in the latter can be attributed to the presence of the electron states of the 2BOC, Si_5 and ≡Si defects in the SiO_2 energy gap, since four-membered rings create only electron states near the top of the valence band, which leads to only a very small decrease in E_g [26]. In the a-SiO_2-4800 and a-SiO_2-4900 structures with an oxygen vacancy, the E_g values are also determined by the presence of corresponding point defects with electron states in the band gap of silicon dioxide in these amorphous structures even before the creation of an oxygen vacancy.

The conformations of two types of oxygen vacancies created by removing one of two oxygen atoms from the $2BO_3C$ defect existing in the stoichiometric a-SiO_2-4500 state are different from the simple Si–Si bond. When the threefold coordinated oxygen atom is removed from $2BO_3C$ (this state is denoted as 4500_2BOC in Tab. 2), the ≡Si defect is formed in a pyramidal conformation near the vacancy, and the 2BOC defect retains its original geometry but without one removed bridging oxygen atom; in particular, the R(Si–Si) distance of 2.49 $\AA$ is almost the same as in the original stoichiometric a-SiO_2-4500 in the $2BO_3C$ defect. The resulting oxygen-deficient center can be interpreted either as two adjacent threefold coordinated silicon atoms with a common oxygen atom, or as two twofold coordinated silicon atoms linked to each other by an oxygen bridge =Si–O–Si=, where symbol "=" designates two Si–O bonds with a regular part of SiO_2 atomic network. When the twofold coordinated oxygen atom is removed from $2BO_3C$ (this state is denoted as 4500_2BOC-1 in Tab. 2), after energy optimization, two Si atoms of the $2BO_3C$ defect remain to be linked by the threefold coordinated oxygen atom, the distance between these silicon atoms decreases to 2.21 $\AA$ indicating strengthening of Si–Si bond between these atoms. This oxygen-deficient center can be interpreted as two twofold coordinated silicon atoms linked to each other by a threefold coordinated oxygen atom.

B. Oxygen vacancy in initial cristobalite + the melting-quenching procedure. An oxygen vacancy is created near the center of the supercell of the initial cristobalite crystal, followed by the melting-quenching procedure to obtain amorphous states at different melt stabilization temperatures T_{melt}. Main characteristics of these amorphous supercells with the initially created oxygen vacancy are presented in Tab. 3.

In a-SiO_2-4600, the atomic network topology is almost the same as in the initial crystal with some deviations of Si–O–Si angles from their crystalline values. However, besides the oxygen vacancy there are three five-membered and one four-membered strained ring. The presence of these rings increases the supercell energy by 4.8 eV (compare E_{opt}(OV) in Tabs. 2 and 3, columns 4600), since stoichiometric a-SiO_2-4600 has only six-membered rings as in the initial crystal. The oxygen vacancy created in the initial crystal keeps its form as a Si–Si bond with R(Si–Si) = 2.32 $\AA$ after the melting-quenching procedure, but its two Si neighbors have changed

Table 3. Characteristics of the amorphous supercell with an oxygen vacancy after the melting-quenching procedure from the initial crystalline supercell

Structure	Oxygen vacancy				
	Amorphous SiO_2, T_{melt}, °K				
	4600	4600-1	4700	4800	4900
E_{opt}(OV), eV	−1504.73	−1488.54	−1506.81	−1473.52	−1486.28
Defects	OV	2BOC, $2BO_3C$, Si_5, ≡Si, –Si–O	OV, 2BOC	2BOC, =Si, ≡Si–O, ≡Si, Si_5	2BOC, =Si–O, ≡Si
R(Si–Si), $\AA$	2.32	–	2.37	–	–
ρ, g/cm^3	2.196	2.172	2.147	2.012	2.058
E_g, eV	4.98	1.99 3.24	5.08	1.87	1.91

their numbers – each atom in the supercell has its own unique number in the list of all atoms in the supercell, which is preserved during MD simulations. This means that the oxygen vacancy changes its position in the supercell during the melting-quenching procedure due to the hopping diffusion of oxygen atoms through the nodes of the SiO_4-network. Two Si atoms adjacent to the vacant site form Si–O bonds with six neighboring oxygen atoms, which are somewhat elongated to 1.64–1.65 $\AA$ compared to the Si–O bonds of 1.62–1.63 $\AA$ in defect-free regions.

An independent run of the melting-quenching procedure gives a new configuration of the amorphous state a-SiO_2-4600-1 with two unpaired electrons. The energy of this state is 16 eV higher than the energy of the a-SiO_2-4600 state obtained during the first run of melting-quenching and having no unpaired electrons, see the 4600 column in Tab. 3. The topology of the atomic network in the amorphous state of a-SiO_2-4600-1 differs significantly from the topology of the weakly disordered arrangement of atoms in a-SiO_2-4600, which is close to topology of cristobalite. In the a-SiO_2-4600-1 state, there are two 2BOC centers, one $2BO_3C$, two fivefold coordinated silicon atoms Si_5, two threefold coordinated silicon atoms ≡Si, and also a twofold coordinated silicon atom, in which one of the neighboring oxygen atoms is non-bridging, and this defect can be designated for brevity as –Si–O. The Si–O bond of the non-bridging atom (1.54 $\AA$) is much shorter than the Si–O bond of a regular bridging oxygen atom (1.62 $\AA$). In the a-SiO_2-4600-1 state, there are also 3-, 4- and 5-membered rings. It is easy to make sure that stoichiometry of this amorphous state is equal to one oxygen vacancy in the supercell. Really, the 2BOC defects do not violate the stoichiometry of SiO_2, two Si_5 defects being combined with two ≡Si defects restore stoichiometry of SiO_2, the $2BO_3C$ is transformed to 2BOC and ≡Si, and the latter being combined with the –Si–O defect gives the twofold coordinated silicon atom =Si, which corresponds to the stoichiometry of one oxygen vacancy in the supercell.

One of the two fivefold coordinated silicon atoms is included into one of the two 2BOC defects. One of the two threefold coordinated silicon atoms ≡Si has a pyramidal conformation. This silicon atom is linked by two Si–O bonds to regular fourfold coordinated silicon atoms, and the oxygen atom of the third Si–O bond is included in the 2BOC defect. The second threefold coordinated atom ≡Si has a planar conformation; it is linked by two Si–O bonds to regular fourfold coordinated silicon atoms and the third Si–O bond forms a bridge with the fivefold coordinated atom Si, which is a part of a 2BOC defect.

Two unpaired electrons are located at two separated defects: at ≡Si with pyramidal conformation and at non-bridging oxygen atom of the –Si–O defect. The former is the so-called paramagnetic E′-center and the latter is a new type of modified Non-Bridging Oxygen Hole Center (NBOHC), both of them are in the list of most common radiation-induced centers in silica glass and in silica-based fibers [5, 15, 17, 18, 28].

In a-SiO_2-4600-1, the values of E_g for excitation of electron with opposite directions of spins are 1.99 and 3.24 eV. The mass density of the a-SiO_2-4600-1 state is 0.024 g/cm^3 lower than density of a-SiO_2-4600.

In a-SiO_2-4700, the a-SiO_2 structure contains one oxygen vacancy, one 2BOC defect, three five-membered and one three-membered strained rings. There are no unpaired electrons in this state. Otherwise, this structure has not lost the ordered crystal topology with some angular disorder. The stoichiometric a-SiO_2-4700 has the SiO_4-network topology as in the initial crystal without the 2BOC defect and 5- and 3-membered rings, with only six-membered rings. The oxygen vacancy keeps its form as a Si–Si bond, but its two Si neighbors have changed again – a pair of other Si atoms have become adjacent to the vacant oxygen site. The distance between Si atoms neighboring to the vacant oxygen site R(Si-Si) is equal to 2.37 $\mathring{A}$.

An increase in the duration of melt stabilization at T_{melt} = 4700 K from 6 ps to 14 ps leads to a strong rearrangement of the topology of the atomic network, appearance of 3-, 4-, and 5-membered rings, an increase in the energy of corresponding a-SiO_2 by more than 26 eV, and the appearance of point defects: five 2BOC defects and two defects =Si–O. The oxygen vacancy has a form of Si–Si bond with R(Si-Si) = 2.31 $\mathring{A}$. The silicon atoms that are neighbors of the oxygen vacancy have changed again – a pair of other Si atoms now appear next to the oxygen vacancy. This is a different pair of atoms comparing with neighbors of the vacancy in the initial crystal and in the amorphous state obtained from the melt stabilized during 6 ps. Values of R(Si-Si) for the oxygen vacancies in a-SiO_2 obtained for T_{melt} = 4600 and 4700 K correspond well to the R(Si-Si) = 2.36 $\mathring{A}$ for the oxygen vacancy in the quartz crystal calculated with a full long-range atomic relaxation by the *ab initio* method [27]. The significantly larger distance R(Si-Si) = 2.48 $\mathring{A}$ obtained for the oxygen vacancy in the initial β-cristobalite crystal after its energy optimization (see Tab. 2) demonstrates the importance of long-range atomic relaxation and disorder for the properties of this defect.

In the =Si–O defect, Si atom is in the plane of its three oxygen neighbors, the lengths of two Si–O bonds are close to those in the defect-free region, and the Si–O bond with the non-bridging oxygen atom is noticeably shorter and is 1.53 $\mathring{A}$. Since there are no unpaired electrons in the system, it can be assumed that one of the valence electrons of the Si atom in such a defect passes to the non-bridging oxygen atom. Due to this, the defect acquires a noticeable dipole moment, and the additional Coulomb attraction of these opposite charges leads to an additional strengthening of the Si–O bond between the silicon atom and the non-bridging oxygen atom and to its shortening. In the obtained amorphous supercell, two =Si–O defects are located far from each other: the distance between corresponding Si atoms equals 6.63 $\mathring{A}$. The pair of =Si–O defects does not violate stoichiometry. Each defect in this pair complements the other, and they both form one 2BOC. Therefore, this pair of =Si–O defects does not relate to oxygen deficiency of the sample, as well as 2BOCs, and the oxygen vacancy is the only ODC in this sample.

At higher melt stabilization temperatures T_{melt} = 4800 and 4900 K, the SiO_4-network with the initial oxygen vacancy loses the ordered topology of the initial crystal, and the oxygen vacancy in the form of a Si–Si bond disappears, possibly due to the mobility of Si atoms in the

melt. In both cases, there are no unpaired electrons, and many small-membered rings, 2BOC defects and pores appear. Besides, several additional point defects can be observed.

In a-SiO_2-4800, there is no oxygen vacancy, and instead the following defects are found: one twofold coordinated silicon atom =Si, two threefold coordinated silicon atoms ≡Si, a fivefold coordinated silicon atom Si_5 and the ≡Si–O defect with a non-bridging oxygen atom. The Si_5 defect is simultaneously a part of the 2BOC center and a part of the strained three-membered ring. One of the threefold coordinated Si atoms is also a part of another 2BOC defect. So, in this amorphous state, only the twofold coordinated silicon atom =Si can be definitely attributed to the oxygen deficiency, because remaining pairs of defects, Si_5 and ≡Si, as well as ≡Si–O and ≡Si, are combined to the perfect stoichiometry of silicon dioxide. In fact, stoichiometry of =Si is the same as an oxygen vacancy. The energy of this supercell is more than 33 eV higher than the energy of the supercell obtained from the melt stabilized at 4700 K for 6 ps (see Tab. 3).

In the a-SiO_2-4900 diamagnetic state, the =Si–O defect with a non-bridging oxygen atom and two threefold coordinated silicon atoms ≡Si can be identified. The ≡Si defects have a pyramidal structure, are separated from each other by a distance of 12.6 $\AA$ and are apparently associated with oxygen deficiency, since they represent two parts of an oxygen vacancy. Note that the presence of defect =Si–O does not violate the stoichiometry of this supercell, since the addition of this defect through its non-bridging oxygen atom to defect ≡Si again yields a defect of the same type, that is, the ≡Si defect. The supercell energy is about 20 eV higher than the energy of the supercell obtained from the melt stabilized at 4700 K for 6 ps.

C. Melting-quenching procedure applied to amorphous supercells with an oxygen vacancy. The optimized oxygen vacancy created in stoichiometric amorphous SiO_2 (see Tab. 2) is subjected to the melting-quenching procedure at the same melt stabilization temperature T_{melt}, that was used in the preparation of the original amorphous stoichiometric state.

All obtained states of amorphous supercells are diamagnetic – there are no unpaired electrons. After the melting-quenching procedure, oxygen vacancies with exotic conformations, created in the $2BO_3C$ defect in the amorphous state a-SiO_2-4500, are transformed into the usual type of oxygen vacancies in the form of a Si–Si bond. In addition to oxygen vacancies, either 2BOC or =Si–O are formed. In the 4500_2BOC-1 state, 5- and 3-membered rings also appear.

In the case of a-SiO_2-4600, there are one 2BOC defect, an oxygen vacancy in the form of Si–Si bond, and 3- and 5-membered rings. In the case of a-SiO_2-4700, there are three 2BOC defect, an oxygen vacancy in the form of Si–Si bond, and three 3- and one 5-membered rings.

After applying the melting-quenching procedure with melt stabilization for 6 ps to the amorphous state of a-SiO_2-4700_19ps obtained by stabilizing the melt at 4700 K for 19 ps with an oxygen vacancy, an amorphous state is obtained containing $2BO_3C$, Si_5 and =Si defects in addition to 2BOC centers and a large number of 3- and 4-membered rings, but without an oxygen vacancy. Here, only twofold coordinated silicon atom =Si can be considered as an oxygen deficient center (ODC). Indeed, the combination of $2BO_3C$ and Si_5 defects can obviously be converted into stoichiometry of defect-free SiO_2: $2BO_3C + Si_5 \rightarrow 2BOC + \equiv Si + Si_5 \rightarrow SiO_2 + \equiv Si–O + \equiv Si$, where a combination of ≡Si and ≡Si–O gives again stoichiometry of defect-free SiO_2.

The main results obtained for the oxygen vacancy are as follows:

1. Despite the dramatic change in some cases of the topology of the atomic network after the melting-quenching procedure, the bulk of silicon dioxide atoms form a network of SiO_4-

tetrahedra connected to each other by their vertices – one common vertex for two adjacent tetrahedra, as in silica glass.

2. An oxygen vacancy is a relatively stable point defect of silicon dioxide. When created in a cristobalite crystal, it retains the Si–Si bond form up to the melt stabilization temperature of 4700 K (for 6 and for 14 ps of melt stabilization). The formation energy of such a vacancy is about 8 eV.
3. At higher melt stabilization temperatures, the vacancy loses its form as a Si–Si bond and is transformed into two threefold coordinated Si atoms located far from each other. This may be due to the diffusion of silicon atoms.
4. The presence of an oxygen vacancy in the original crystal can even lead to a strong rearrangement of the topology of the atomic network after the melting-quenching procedure even at such a low melt stabilization temperature as 4600 K when a corresponding stoichiometric supercell retains the atomic network topology of the initial crystal.
5. The presence of an oxygen vacancy in the original crystal promotes formation of other defects as a result of obtaining an amorphous state using the melting-quenching procedure compared to the amorphous state of the stoichiometric supercell. These are the same defects that are presented in stoichiometric samples of amorphous silicon dioxide: 2BOC defects, threefold and fivefold coordinated silicon atoms, ≡Si and Si_5, =Si–O defects with a non-bridging oxygen atom, threefold coordinated oxygen atom O_3, as well as 3-, 4- and 5-membered strained rings.
6. Due to stochastic nature of the MD simulation, independent runs of the melting-quenching procedure can lead to amorphous states with different atomic network topology and different set of point defects.
7. ESR-active states with unpaired electrons have significantly higher energies than diamagnetic states in the studied amorphous states of SiO_2.

2.3. Two Separated in Space Oxygen Vacancies, OV+OV

A. Two separated in space oxygen vacancies are created in existing stoichiometric states. By creating two such oxygen vacancies in either crystalline or amorphous supercells and then optimizing the supercell energy, it is easy to show that in all cases the formation energy of two vacancies is approximately twice the formation energy 8 eV of one vacancy found above. The lowest excitation energy of electrons for supercells without other defects corresponds to the excitation energy of one oxygen vacancy obtained above. By creating two oxygen vacancies by removing two oxygen atoms from the $2BO_3C$ center present in a-SiO_2-4500, the following new defect is obtained. This defect consists of two adjacent oxygen vacancies sharing a silicon atom, which is linked to the rest of the atomic network by two Si–O bonds. Of the two other silicon atoms adjacent to the vacancies, one is also linked to the rest of the atomic network by two Si–O bonds and the second one is linked to the atomic network by three Si–O bonds and corresponding distances R(Si–Si) are equal to 2.36 and 2.46 $\AA$, respectively. A characteristic feature of this defect is the very low excitation energy of electrons, 0.22 eV.

B. Two separated oxygen vacancies in initial cristobalite + the melting-quenching procedure. The separated oxygen vacancies OV+OV are created near the center of the supercell of the initial cristobalite crystal, followed by the melting-quenching procedure to obtain amorphous states at different melt stabilization temperatures T_{melt} from 4600 to 4900 K. At T_{melt} = 4600 K, in the oxygen-deficient amorphous state, two separate oxygen vacancies of

the Si–Si bond type are retained. At higher T_{melt}, higher energy amorphous states of the supercell (more than 16 eV) are obtained, in which there are either no oxygen vacancies at all, or there is only one oxygen vacancy, but there is a twofold coordinated silicon atom =Si and other defects that we have already considered. For example, the energy of the amorphous supercell obtained at T_{melt} = 4700 K, which contains one =Si defect, two ≡Si defects, and one 2BOC center, is 16 eV higher than the energy of the amorphous supercell obtained at T_{melt} = 4600 K, which contains only two oxygen vacancies. Comparing the energies of these amorphous supercells, we can conclude that the energy of formation of the =Si defect is significantly greater (by 10–12 eV) than the energy of formation of an oxygen vacancy.

It should be noted that independent runs of the melting-quenching procedure with the same parameters can result in amorphous states that differ greatly in energy and in the composition of point defects. For example, with one run of melting-quenching at T_{melt} = 4700 K of the initial crystal with two oxygen vacancies, a-SiO_2-4700 is obtained with the following point defects: one =Si, two ≡Si and one 2BOC. When re-starting the melting-quenching with the same T_{melt}, we obtain the amorphous state of a-SiO_2-4700-1 with a supercell energy exceeding the supercell energy of the state of a-SiO_2-4700 by 9.3 eV and containing a different set of defects: three ≡Si, one Si_5, one 2BOC, one $2BO_3C$ and one oxygen vacancy of a special type OV′, and in both amorphous states there are no unpaired electrons. The oxygen vacancy OV′ of the Si–Si bond type present here has a peculiarity: one of the silicon atoms adjacent to the vacant site has three bonds with neighboring oxygen atoms, and the second silicon atom has four Si–O bonds. Despite this feature, the Si–Si bond length in this vacancy is 2.44 $\AA$, which is close to the values of ordinary oxygen vacancies with two threefold coordinated neighboring silicon atoms. It is easy to verify that in the a-SiO_2-4700-1 state, the oxygen deficiency of two initial oxygen vacancies is maintained. Indeed, $2BO_3C \rightarrow 2BOC + \equiv Si$, where the 2BOC center does not violate the stoichiometry of SiO_2, and the ≡Si defect together with Si_5 also does not violate the stoichiometry of SiO_2; two ≡Si defects correspond to the stoichiometry of one oxygen vacancy, and the oxygen vacancy OV′ can be decomposed into an ordinary oxygen vacancy OV and a ≡Si–O defect, which together with the remaining third ≡Si defect gives the stoichiometry of defect-free SiO_2.

In both amorphous states of a-SiO_2-4700 and a-SiO_2-4700-1, 3-, 4- and 5-membered rings are present, which, like the 2-membered rings of 2BOC, do not violate the stoichiometry of SiO_2.

At T_{melt} = 4800 and 4900 K, even higher-energy amorphous oxygen-deficient states are obtained, in which various sets of the SiO_2 defects already described above are present.

C. Melting-quenching procedure applied to amorphous supercells with two separated oxygen vacancies. Let us see, what happens if supercells of some amorphous states (see Tab. 1) with a created two oxygen vacancies are again subjected to the melting-quenching procedure. For this purpose, four states with two oxygen vacancies were chosen: three of them are a-SiO_2-4600, a-SiO_2-4700 and a-SiO_2-4800 with two oxygen vacancies separated in space, and the fourth state is a-SiO_2-4500 with two vacancies created by removing two oxygen atoms from the $2BO_3C$ defect, which we designated as a-SiO_2-4500_2BOC. Here, in the melting-quenching procedure, all melts were stabilized within 6 ps. The energies of the supercells of all the obtained amorphous states are significantly higher than the energies of most of the amorphous states with a deficit of two oxygen atoms that we have previously considered, and basically they contain only the defects that we have already considered, but in two cases new defects were encountered.

After melting-quenching, the a-SiO_2-4500_2BOC system with two oxygen vacancies initially created in the $2BO_3C$ defect has no unpaired electrons, and it contains two twofold coordinated silicon atoms =Si, one =Si–O defect with a non-bridging oxygen atom, one Si_5, several 2BOC centers, 3-, 4- and 5-membered rings, and a center that we designate as Di-$2BO_3C$ – a double $2BO_3C$ center (Fig. 2).

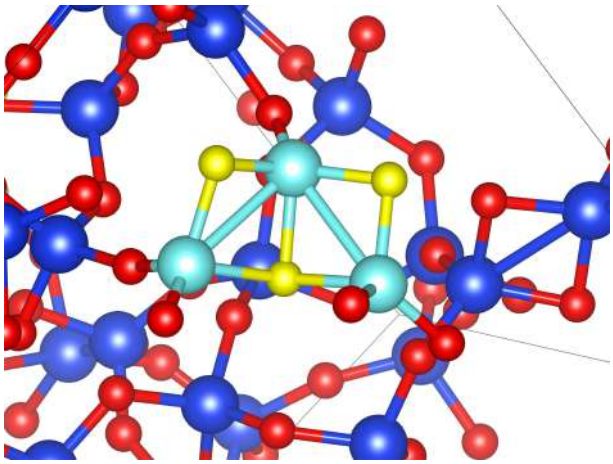

Figure 2. Defect Di-$2BO_3C$ found in a-SiO_2-4500; light blue and yellow balls are Si and O atoms, respectively, which make up the Di-$2BO_3C$ defect

The Di-$2BO_3C$ defect involves three silicon atoms and three oxygen atoms connecting them, and one of these three oxygen atoms, common to two $2BO_3C$ defects, forms three Si–O bonds with the neighboring Si atoms included in this defect. Note that the stoichiometry of the Di-$2BO_3C$ defect is equivalent to the stoichiometry of the threefold coordinated silicon atom ≡Si, which together with Si_5 does not violate the stoichiometry of SiO_2. The defect =Si–O does not violate the stoichiometry of defect-free SiO_2, since it can be broken down into an oxygen atom and a twofold coordinated silicon atom =Si, the stoichiometry of which is equivalent to the stoichiometry of an oxygen vacancy, adding to which the remaining oxygen atom, we obtain the stoichiometry of defect-free SiO_2. Thus, the stoichiometry of the considered amorphous state with two oxygen vacancies and after melting-quenching with a melt stabilization temperature of T_{melt} = 4500 K corresponds to two oxygen vacancies in the supercell, since the stoichiometry of two defects =Si is equivalent to the stoichiometry of two oxygen vacancies.

An independent run of melting-quenching at T_{melt} = 4500 K led to a new, slightly lower in energy (by 3.3 eV), amorphous state with a different set of intrinsic defects, among which there is again the Di-$2BO_3C$ defect, shown in Fig. 2.

Another previously unseen defect, designated by us as the 2BOC′ center, was obtained by applying the melting-quenching procedure to a-SiO_2-4800, in which two oxygen vacancies were created, separated apart in space. The 2BOC′ center is a 2BOC center in which one of the silicon atoms has not two Si–O bonds with the rest of the atomic network, but only one, i.e., it is a threefold coordinated silicon atom atom embedded in a 2BOC center. In this relatively high-energy amorphous state with two unpaired electrons, in addition to the two 2BOC′ centers, the following defects already discovered are also present: one oxygen vacancy OV, a =Si–O defect with a non-bridging oxygen atom, two Si_5 defects, two $2BO_3C$ defects, several 2BOC defects, and 3-, 4-, and 5-membered rings.

2.4. Oxygen di-Vacancy, OdV

The OdV defect can be created in a regular SiO_2-network, crystal or amorphous, by eliminating two oxygen atoms bound to the same Si atom. The oxygen deficiency is the same in both cases, OdV and two separated oxygen vacancies VO+VO: each supercell is missing two oxygen atoms.

A. The OdV defect is created in existing stoichiometric states. OdV is created in the cristobalite crystal and in a-SiO_2 prepared from this crystal using several melt stabilization temperatures T_{melt} (4600–4900 K): two oxygen atoms bonded to the same silicon atom are removed, and the energy of the supercell is optimized by varying positions of all atoms, form and volume of the supercell. E_{form}(OdV) is the formation energy of the OdV defect calculated as follows: $E_{form}(OdV) = E_{opt}(OdV) + 2\times E(O) - E_{opt}$, where E_{opt} is the optimized energy of the stoichiometric supercell (see Tab. 1), and $E(O) = -1.897$ eV is determined above just before Tab. 2.

In cristobalite, the OdV defect is in the configuration of two oxygen vacancies in the form of Si–Si bonds of the length 2.61 $\AA$ with a common Si atom, which is linked to the rest of the atomic network by only two Si–O bonds (Fig. 3).

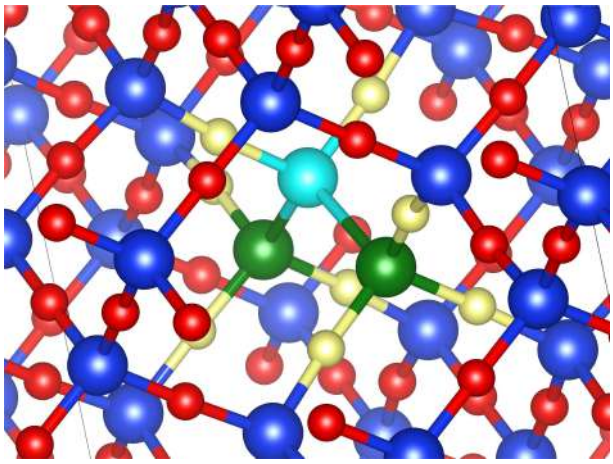

Figure 3. The OdV defect in cristobalite after the energy optimization

In Fig. 3, the light blue ball is a Si atom with two Si-O bonds; green balls are Si atoms with three Si-O bonds each, yellow balls are oxygen atoms bonded to blue and green Si atoms.

In addition to the restrictions imposed on the relaxation of the atoms of this defect by the atoms of its crystalline environment, each of the two neighboring threefold coordinated silicon atoms ≡Si restricts the relaxation of the third Si atom to the second neighboring threefold coordinated silicon atom. This is the reason why Si–Si distances in these two vacancies are noticeably larger than the R(Si–Si) = 2.48 $\AA$ in the single oxygen vacancy in cristobalite (see Tab. 2). In amorphous states, the Si–Si distances in the two adjacent oxygen vacancies are in the range 2.4–2.6 $\AA$. The formation energy of the OdV defect is close to twice the formation energy of a single oxygen vacancy (see Tab. 2).

Having created OdV in cristobalite and in defect-free a-SiO_2-4600 and a-SiO_2-4700 amorphous states, we determine the lowest energy of electronic excitations for these states E_g, equal to 4.20, 4.46 and 4.47 eV, respectively. These values are considerably lower E_g of a single oxygen vacancy and of defect-free amorphous systems, see Tab. 2 and Tab. 1, respectively. This

indicates that the optical excitation energy of the OdV defect is significantly less than the excitation energy of a single oxygen vacancy. Taking into account the known underestimation of the E_g values in the PBE calculations [8], we can assume that our results qualitatively correspond to the assignment of the experimentally observed absorption bands in quartz glass at 7.6 eV and 5.0 eV to a single oxygen vacancy and to an oxygen divacancy OdV.

B. The OdV defect in initial cristobalite + the melting-quenching procedure. Let us consider what happens to the oxygen divacancy created in cristobalite after the melting-quenching amorphization procedure at different melt stabilization temperatures T_{melt}.

The initially created in the crystal oxygen divacancy OdV is not preserved as a result of the melting-quenching procedure at T_{melt} = 4600 K, and other defects arise in its place. Two fivefold coordinated silicon atoms Si_5 and a new diamagnetic defect OdV′ shown in Fig. 4 are formed.

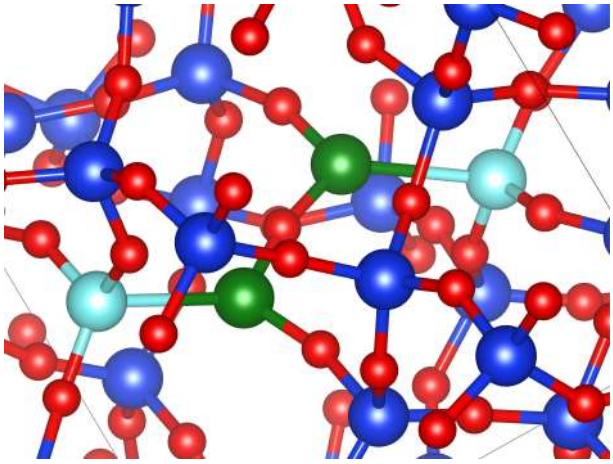

Figure 4. The OdV′ center appeared in a-SiO_2-4600 after the melting-quenching procedure from the initial β-cristobalite with OdV

In Fig. 4, the green balls are silicon atoms neighbors of oxygen vacancies which bound the vacancies by a Si–O–Si bridge; the light blue balls are silicon atoms that link oxygen vacancies to the rest of a-SiO_2 network; blue and red balls are fourfold and twofold coordinated Si and O atoms, respectively, forming the a-SiO_2 network.

The OdV′ defect consists of two adjacent oxygen vacancies linked to each other by a Si–O–Si bridge, in which each silicon atom, a part of Si–Si bond of OV, participates in only two Si–O bonds. For brevity, we denote this defect as modified oxygen divacancy OdV′. Topology of the atomic network has changed somewhat compared to the crystal – two three-membered rings have appeared.

When melting-quenching is repeated at T_{melt} = 4600 K, a state with two unpaired electrons is obtained, and its energy is higher than the previous state of a-SiO_2-4600 by approximately 15 eV. In this case, instead of two Si_5 defects and an OdV′ defect, there is an oxygen vacancy with R(Si-Si) = 2.39 $\AA$, two ≡Si defects with a pyramidal conformation, a =Si–O defect with a non-bridging oxygen atom, and two 2BOC centers. Of course, there are also 3-, 4- and 5-link rings. It is easy to verify that these defects do not change the degree of oxygen deficiency, which remains as it was before melting-quenching – one oxygen divacancy OdV per supercell. Indeed, by breaking two Si–Si bonds, the OdV′ defect can be represented as two twofold coordinated

silicon atoms =Si and two threefold coordinated silicon atoms ≡Si; the combination of two ≡Si with two Si_5 gives a defect-free stoichiometry of SiO_2, so that two =Si defects remain, corresponding to an oxygen deficiency of two oxygen atoms per supercell.

In other amorphous states obtained at T_{melt} = 4700, 4800 and 4900 K, different sets of point defects described above are formed, but energies of these states are more than 13 eV greater than the energy of a-SiO_2-4600 with two Si_5 and OdV′. There are neither OdV, nor OdV′ in these high energy amorphous states, but other defects are presented. Most of these defects were described above, but a new defect =Si–O–Si= is found in a-SiO_2-4800, which is two threefold coordinated silicon atoms linked to each other by a common oxygen atom (Fig. 5). In this defect, silicon atoms are located so close to each other that a strong Si–Si bond is formed between them, the length of which is 2.19 $\mathring{A}$, and due to this approaching, the Si–O–Si angle of the oxygen bridge between these atoms is close to a right angle.

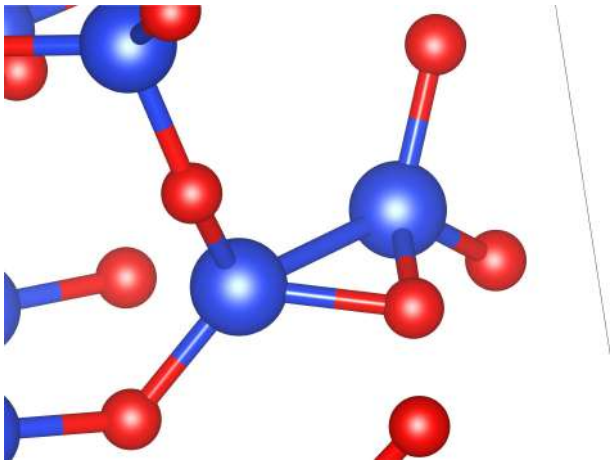

Figure 5. Defect =Si–O–Si= found in a-SiO_2-4800 with the oxygen deficiency of oxygen divacancy

This new defect can be interpreted as a 2BOC center without one oxygen bridge, but with the geometry of the remaining atoms almost like in the 2BOC center. In addition to the =Si–O–Si= defect, there are also OV, =Si–O, several 2BOC and 3-, 4- and 5-membered rings in such a-SiO_2-4800. The =Si–O–Si= defect can be obviously named as Oxygen Deficient Center (ODC) corresponding to the stoichiometry of an oxygen vacancy.

C. Melting-quenching procedure applied to amorphous supercells with OdV. When supercells of some amorphous states with a hand created OdV defect are again subjected to the melting-quenching procedure with T_{melt} = 4600, 4700 and 4800 K, new amorphous states are obtained with defects described above: =Si, OV, =Si–O, ≡Si–O, $2BO_3C$, Si_5, ≡Si, and OdV.

The main results obtained for the oxygen divacancy OdV are as follows. The oxygen divacancy OdV is unstable with respect to the melting-quenching procedure at all studied melt stabilization temperatures and decomposes into other defects. The lowest-energy of these defects is the OdV′ center, formed by two adjacent oxygen vacancies linked by a Si–O–Si bridge, in which each Si atom participates in only two Si–O bonds (Fig. 4). This defect is formed at T_{melt} = 4600 K. At higher melt stabilization temperatures, spatially separated oxygen vacancies, threefold coordinated silicon atoms ≡Si, and twofold coordinated silicon atoms =Si appear.

3. Discussion

Based on the conducted studies of numerous (more than 35) amorphous states of silicon dioxide obtained by the melting-quenching procedure from a crystal, the following main results can be summarized and discussed. The density of the obtained a-SiO_2 samples is close to the experimentally measured value of 2.2 g/cm^3 and is in the range 1.91–2.26 g/cm^3. Among all possible intrinsic point defects, the first to appear at the lowest melt stabilization temperatures T_{melt} are the 2BOC or 2BO_3C centers. This means that the formation energy of such defects is the lowest compared to other intrinsic defects in silica. The 2BOC defect is two SiO_4-tetrahedra linked by two oxygen vertices, and the 2BO_3C defect is a modification of it. This was first shown in stoichiometric a-SiO_2 using spin-unpolarized quantum molecular dynamics simulations in [22, 24] and confirmed in stoichiometric and oxygen-deficient a-SiO_2 using spin-polarized simulations in the present work. The number of such defects increases with increasing T_{melt}, but does not exceed several defects per supercell containing 192 atoms. The 2BOC centers do not violate stoichiometry of SiO_2.

For cristobalite and quartz crystals, the point defects and amorphization occur at T_{melt} between 4500 and 4700 K with the parameters of the melting-quenching procedure used: heating and cooling rates of 0.5 K/fs and melt stabilization of several picoseconds. The term "amorphization" refers to a change in the topology of the atomic network of crystalline SiO_2 with fourfold coordinated Si atoms and twofold coordinated oxygen atoms, which results in the formation of rings consisting of a small number (3, 4, 5) of Si–O–Si bridges. For a stishovite crystal with sixfold coordinated Si atoms and threefold coordinated oxygen atoms, amorphization occurs at significantly lower melt stabilization temperatures T_{melt} of about 3000 K, with the same parameters of the melting-quenching procedure. In general, the topology of atomic network of amorphous silica obtained from stishovite is similar to the topology of a-SiO_2 obtained from cristobalite or quartz.

With increasing time of the melting-quenching procedure, for example, with increasing time of melt stabilization, the critical value T_{melt}, above which amorphization occurs, decreases. The presence of vacancies or divacancies in the original crystal promotes the formation of point defects in the amorphous silicon dioxide obtained by melting-quenching and causes a change in the topology of the atomic network compared to the crystal at lower melt stabilization temperatures.

Despite the radical change in the topology of the atomic network during amorphization using melting-quenching, the bulk of the silicon dioxide atoms form a network of SiO_4-tetrahedra, connected to each other by their vertices - one common vertex for two adjacent tetrahedra, as in quartz glass. Most of the point defects - the local disruption of this network - found in the stoichiometric a-SiO_2 models are also present in oxygen-deficient a-SiO_2. The use of spin-polarized calculations in the melting-quenching procedure leads to the discovery of new point defects that are not obtained in spin-unpolarized calculations, in particular, ESR-active point defects with unpaired electrons. The energy of the diamagnetic states of a-SiO_2 is significantly lower than the energy of ESR-active states containing defects with unpaired electrons.

The following intrinsic point defects are found in stoichiometric a-SiO_2: 2BOC, 2BO_3C in which one oxygen atom of the 2BOC defect has a third Si–O bond linking it to the rest of the atomic network, the ≡Si–O and =Si–O defects with non-bridging oxygen atoms, a threefold coordinated silicon atom ≡Si, a fivefold coordinated silicon atom Si_5, a twofold coordinated silicon atom =Si, an oxygen vacancy OV and a threefold coordinated oxygen atom O_3. All these defects are also found in oxygen-deficient a-SiO_2.

In the present work, oxygen deficient a-SiO_2 was prepared by removing one or two oxygen atoms from a supercell containing 64 Si and 128 O atoms, combined with a melting-quenching procedure. In oxygen-deficient a-SiO_2, apart from defects of stoichiometric a-SiO_2, the following additional point defects were obtained: a 2BOC′ defect, in which one silicon atom has only three Si–O bonds, a Di-2BO_3C defect, which is two combined 2BOC defects with one common silicon atom and one common oxygen atom, the latter forms three Si–O bonds with three silicon atoms that make up this defect, a =Si–O–Si= defect, which is two threefold coordinated silicon atoms linked to each other by a common oxygen atom, a modified oxygen vacancy OV′, in which one of the Si atoms adjacent to the vacant site has three bonds with neighboring oxygen atoms, and the second Si atom has four Si–O bonds, an oxygen divacancy OdV, a modified oxygen divacancy OdV′, and a –Si–O defect, which is a silicon atom with two Si–O bonds, one bond links this atom to the rest of atomic network and another bond links this silicon atom with a non-bridging oxygen atom. For clarity, we have presented all the defects we discovered in Tab. 4.

Table 4. Intrinsic defects discovered in various amorphous states of SiO_2 in our simulation

Silicon dioxide amorphous states	Point defects
Stoichiometric a-SiO_2	2BO_3C, ≡Si–O, Si_5, ≡Si, O_3, 2BOC, =Si, OV, =Si–O
Oxygen-deficient a-SiO_2, Single oxygen vacancy	OV, Si_5, ≡Si, O_3, 2BOC, 2BO_3C, =Si, =Si–O, –Si–O
Oxygen-deficient a-SiO_2, Two spatially separated oxygen vacancies	OV, Si_5, ≡Si, 2BOC, 2BO_3C, =Si, =Si–O, O_3, Di-2BO_3C, 2BOC′, OV′
Oxygen-deficient a-SiO_2, Single oxygen divacancy	OV, OdV, Si_5, ≡Si, 2BOC, 2BO_3C, =Si, =Si–O, ≡Si–O, OdV′, =Si–O–Si=

Comparing the sets of defects in different rows of Tab. 4, we can conclude that the following 16 point defects are found in oxygen-deficient a-SiO_2: nine defects 2BOC, 2BO_3C, ≡Si–O, =Si–O, ≡Si, =Si, Si_5, OV, O_3, which are also found in stoichiometric a-SiO_2, and seven defects –Si–O, Di-2BO_3C, 2BOC′, =Si–O–Si=, OV′, OdV, and OdV′, which are found only in oxygen-deficient a-SiO_2. Not all of these sixteen defects are associated with local oxygen deficiency. The Si_5, 2BOC, and ≡Si–O defects present in our models of stoichiometric and oxygen-deficient a-SiO_2 are obviously not oxygen-deficient centers. The =Si–O defect is also not an oxygen-deficient center. Indeed, the =Si–O defect can be decomposed into the twofold coordinated silicon atom =Si and an oxygen atom, the stoichiometry of =Si is equal to the stoichiometry of an oxygen vacancy, which in turn combines with an oxygen atom, resulting in the formation of stoichiometric silicon dioxide. Consequently, we can conclude that we have discovered the following 12 intrinsic point defects in a-SiO_2 associated with oxygen deficiency: OV, OV′, =Si, ≡Si, OdV, OdV′, =Si–O–Si=, 2BO_3C, Di-2BO_3C, 2BOC′, O_3 and –Si–O. Note that the latter, together with the ≡Si defect, produces a twofold coordinated silicon atom =Si, which also represents an oxygen-deficient center, corresponding in stoichiometry to the oxygen vacancy OV. Also, the stoichiometry of the O_3 defect coincides with the stoichiometry of the ≡Si defect, and therefore the O_3 defect can be considered to be associated with oxygen deficiency, just like

the ≡Si defect. To avoid confusion, we emphasize that in existing publications, oxygen-deficient centers (ODCs) are non-paramagnetic defects with specific optical characteristics, and until now, either an oxygen vacancy OV or a twofold coordinated silicon atom =Si have been considered as models of these centers. In this paper, we take a broader approach and refer to any defects caused by local oxygen deficiency as oxygen-deficient centers.

In this study, we did not detect the so-called peroxy bridge (linkage) in any amorphous state. This defect has long been discussed in the scientific literature as a precursor to the radiation-induced paramagnetic peroxy radical [4, 7, 9, 20]. In [24], this defect was discovered in the amorphous state of a-SiO_2-5000, obtained by simulating the melting-quenching of an alpha-quartz crystal using spin-unpolarized calculations. Clarification of the reasons for its absence in the amorphous states obtained in this work requires further research.

An estimate of the formation energy of a twofold coordinated silicon atom =Si is given, according to which the formation energy of this defect is significantly greater, by 10–12 eV, than the formation energy of an oxygen vacancy, equal to 8 eV. Moreover, a comparison of the supercell energies of all the amorphous states we studied showed that twofold coordinated silicon atoms =Si are present only in high-energy states along with other defects.

The total CPU time for the entire melting-quenching procedure at T_{melt} = 4700 K is 11.22 days on the Lomonosov-2 supercomputer. In total, more than 35 melting-quenching procedures were carried out during the present research, which took more than 1 year CPU time on Lomonosov-2.

Conclusion

The conducted modeling revealed the configurations of possible intrinsic point defects in amorphous silicon dioxide, and along with the known ones, oxygen vacancies, twofold coordinated silicon atoms =Si, E′-centers and NBOHC, new defects were also identified, including defects associated with oxygen deficiency. A total of twelve defects associated with local oxygen deficiency were identified. Many of the defects found have electronic states in the band gap of silicon dioxide, which can lead to absorption bands in the transparency window of defect-free SiO_2, including the visible and near-IR ranges. Such defects can significantly affect the laser damage threshold of optical coatings using amorphous silicon dioxide layers, as well as radiation-induced absorption in silica-based optical fibers and leakage currents in various semiconductor devices using silicon dioxide as insulating layers. The defects found can become a broad basis for interpreting experimental data from optical and ESR measurements. Many new defects described in the present work for the first time are found due to using quantum molecular dynamics through the whole melting-quenching procedure in the spin-polarized approach. A more accurate description of the optical characteristics of the detected defects requires separate studies, including other more accurate methods for calculating electron excitations. The simulation technique used in this work can also be applied to model a wide range of impurity defects in silicon dioxide, which play an important role in both fiber optics and multilayer optical coatings.

Acknowledgments

The study was conducted under the state assignment of Lomonosov Moscow State University.

The research was carried out using the equipment of the shared research facilities of HPC computing resources at Lomonosov Moscow State University, including the Lomonosov-2 supercomputer [29].

References

1. Dianov, E.M., Kornienko, L.S., Nikitin, E.P., *et al.*: Radiation-optical properties of quartz glass fiber-optic waveguides (review). Soviet Journal of Quantum Electronics 13(3), 274 (1983). https://doi.org/10.1070/QE1983v013n03ABEH004145

2. DiStefano, T.H., Eastman, D.E.: The band edge of amorphous SiO_2 by photoinjection and photoconductivity measurements. Solid State Communications 9(24), 2259–2261 (1971). https://doi.org/10.1016/0038-1098(71)90643-0

3. Feigl, F.J., Fowler, W., Yip, K.L.: Oxygen vacancy model for the E_1' center in SiO_2. Solid State Communications 14(3), 225–229 (1974). https://doi.org/10.1016/0038-1098(74)90840-0

4. Friebele, E.J., Griscom, D.L., Stapelbroek, M., Weeks, R.A.: Fundamental defect centers in glass: The peroxy radical in irradiated, high-purity, fused silica. Physical Review Letters 42, 1346–1349 (1979). https://doi.org/10.1103/PhysRevLett.42.1346

5. Griscom, D.L.: Defect structure of glasses: Some outstanding questions in regard to vitreous silica. Journal of Non-Crystalline Solids 73(1), 51–77 (1985). https://doi.org/10.1016/0022-3093(85)90337-0

6. Griscom, D.L.: A minireview of the natures of radiation-induced point defects in pure and doped silica glasses and their visible/near-IR absorption bands, with emphasis on self-trapped holes and how they can be controlled. Physics Research International 2013(1), 379041 (2013). https://doi.org/10.1155/2013/379041

7. Griscom, D.L., Mizuguchi, M.: Determination of the visible range optical absorption spectrum of peroxy radicals in gamma-irradiated fused silica. Journal of Non-Crystalline Solids 239(1), 66–77 (1998). https://doi.org/10.1016/S0022-3093(98)00721-2

8. Hafner, J.: *Ab-initio* simulations of materials using VASP: Density-functional theory and beyond. Journal of Computational Chemistry 29(13), 2044–2078 (2008). https://doi.org/10.1002/jcc.21057

9. Kitagawa, I., Maruizumi, T.: New intrinsic pair defects in silicon dioxide interface. Applied Surface Science 216(1), 264–269 (2003). https://doi.org/10.1016/S0169-4332(03)00379-9

10. Kresse, G., Furthmüller, J.: Efficient iterative schemes for *ab initio* total-energy calculations using a plane-wave basis set. Physical Review B 54, 11169–11186 (1996). https://doi.org/10.1103/PhysRevB.54.11169

11. Kresse, G., Joubert, D.: From ultrasoft pseudopotentials to the projector augmented-wave method. Physical Review B 59, 1758–1775 (1999). https://doi.org/10.1103/PhysRevB.59.1758

12. Marsman, M., Paier, J., Stroppa, A., Kresse, G.: Hybrid functionals applied to extended systems. Journal of Physics: Condensed Matter 20(6), 064201 (2008). https://doi.org/10.1088/0953-8984/20/6/064201

13. Shiga, M., Hirata, A., Onodera, Y., Masai, H.: Ring-originated anisotropy of local structural ordering in amorphous and crystalline silicon dioxide. Communications Materials 4(1), 91 (2023). https://doi.org/10.1038/s43246-023-00416-w

14. Skuja, L.: Optical properties of defects in silica. In: Pacchioni, G., Skuja, L., Griscom, D.L. (eds.) Defects in SiO_2 and Related Dielectrics: Science and Technology. pp. 73–116. Springer Netherlands, Dordrecht (2000). https://doi.org/10.1007/978-94-010-0944-7_3

15. Skuja, L., Tanimura, K., Itoh, N.: Correlation between the radiation-induced intrinsic 4.8 eV optical absorption and 1.9 eV photoluminescence bands in glassy SiO_2. Journal of Applied Physics 80(6), 3518–3525 (1996). https://doi.org/10.1063/1.363224

16. Skuja, L.: Optically active oxygen-deficiency-related centers in amorphous silicon dioxide. Journal of Non-Crystalline Solids 239(1), 16–48 (1998). https://doi.org/10.1016/S0022-3093(98)00720-0

17. Skuja, L., Kajihara, K., Grube, J., Hosono, H.: Luminescence of non-bridging oxygen hole centers in crystalline SiO_2. AIP Conference Proceedings 1624(1), 130–134 (2014). https://doi.org/10.1063/1.4900468

18. Skuja, L., Kajihara, K., Hirano, M., Hosono, H.: Visible to vacuum-UV range optical absorption of oxygen dangling bonds in amorphous SiO_2. Physical Review B 84, 205206 (2011). https://doi.org/10.1103/PhysRevB.84.205206

19. Skuja, L., Streletsky, A., Pakovich, A.: A new intrinsic defect in amorphous SiO_2: Twofold coordinated silicon. Solid State Communications 50(12), 1069–1072 (1984). https://doi.org/10.1016/0038-1098(84)90290-4

20. Sokolov, V.O., Sulimov, V.B.: Semi-empirical calculation of peroxy linkage in vitreous silicon dioxide. Physica Status Solidi (B) 142(1), K7–K12 (1987). https://doi.org/10.1002/pssb.2221420134

21. Strand, J., Kaviani, M., Gao, D., *et al.*: Intrinsic charge trapping in amorphous oxide films: status and challenges. Journal of Physics: Condensed Matter 30(23), 233001 (2018). https://doi.org/10.1088/1361-648X/aac005

22. Sulimov, A.V., Kutov, D.C., Grigoriev, F.V., *et al.*: Generation of amorphous silicon dioxide structures via melting-quenching density functional modeling. Lobachevskii Journal of Mathematics 41(8), 1581–1590 (2020). https://doi.org/10.1134/S1995080220080193

23. Sulimov, V.B., Sokolov, V.O., Dianov, E.M., Poumellec, B.: Photoinduced structural transformations in silica glass: the role of oxygen vacancies in the mechanism of formation of refractive-index gratings by UV irradiation of optical fibres. Quantum Electronics 26(11), 988 (1996). https://doi.org/10.1070/QE1996v026n11ABEH000857

24. Sulimov, V., Kutov, D., Sulimov, A., *et al.*: Density functional modeling of structural and electronic properties of amorphous high temperature oxides. Journal of Non-Crystalline Solids 578, 121170 (2022). https://doi.org/10.1016/j.jnoncrysol.2021.121170

25. Sulimov, V., Sokolov, V.: Cluster modeling of the neutral oxygen vacancy in pure silicon dioxide. Journal of Non-Crystalline Solids 191(3), 260–280 (1995). https://doi.org/10.1016/0022-3093(95)00293-6

26. Sulimov, V., Kutov, D., Sulimov, A., *et al.*: Study of the anomalous behavior of the a-HFO_2 refractive index with increasing Si doping by quantum molecular dynamics simulation. Journal of the Optical Society of America B 40(10), 2643–2649 (2023). https://doi.org/10.1364/JOSAB.500520

27. Sulimov, V.B., Sushko, P.V., Edwards, A.H., *et al.*: Asymmetry and long-range character of lattice deformation by neutral oxygen vacancy in α-quartz. Physical Review B 66, 024108 (2002). https://doi.org/10.1103/PhysRevB.66.024108

28. Sushko, P.V., Mukhopadhyay, S., Mysovsky, A.S., *et al.*: Structure and properties of defects in amorphous silica: new insights from embedded cluster calculations. Journal of Physics: Condensed Matter 17(21), S2115 (2005). https://doi.org/10.1088/0953-8984/17/21/007

29. Voevodin, V.V., Antonov, A.S., Nikitenko, D.A., *et al.*: Supercomputer Lomonosov-2: Large scale, deep monitoring and fine analytics for the user community. Supercomputing Frontiers and Innovations 6(2), 4–11 (2019). https://doi.org/10.14529/jsfi190201

30. Weinberg, Z.A., Rubloff, G.W., Bassous, E.: Transmission, photoconductivity, and the experimental band gap of thermally grown SiO_2 films. Physical Review B 19, 3107–3117 (1979). https://doi.org/10.1103/PhysRevB.19.3107

31. Yuan, X., Cormack, A.N.: Efficient algorithm for primitive ring statistics in topological networks. Computational Materials Science 24(3), 343–360 (2002). https://doi.org/10.1016/S0927-0256(01)00256-7